A Method of Damage Mechanics Analysis for Solder Material*

H. Eliot Fang[1], C. L. Chow[2] and Fan Yang[2]

[1]Computational Physics and Mechanics Department, Sandia National Laboratories
Albuquerque, New Mexico 87185-0820, U.S.A.

[2]Department of Mechanical Engineering, The University of Michigan-Dearborn
Dearborn, Michigan 48128-1491, U.S.A.

Keywords: Damage Mechanics, Solder Joints, Eutectic Sn-Pb Materials

ABSTRACT

This paper presents a method of damage mechanics analysis for solder joint material stressed to extensive plastic deformation. The material chosen for the current work is the 60Sn-40Pb eutectic alloy due to its wide use. The analysis is based on the thermodynamic theory of irreversible processes. With the introduction of a set of internal state variables, known as damage variables, and a damage effect tensor, a damage dissipative potential function is proposed to enable the formulation of the constitutive equations of elasticity and plasticity coupled with damage. The equations of damage evolution are also derived to monitor damage initiation and growth. Before a damage analysis can be performed with a finite element analysis, the mechanical properties of the chosen solder joint material and its damage variables must first be determined. A method of experimental analysis was developed and used to successfully measure the highly strain sensitive 60Sn-40Pb solder material. The measured properties are presented and various characteristics of the solder material are examined and discussed.

1. INTRODUCTION

Driven by the desire for miniaturization and increased circuit speed, surface mount technology (SMT) has been widely adopted in electronic packaging. However, SMT also brings with it a new era of joint failures. A major finding from mechanical tests is that the joint material, which is responsible for both electrical and mechanical connections, does not have adequate capability to sustain the cyclic mismatch of thermal expansions between the chip carrier (CC) and the printed wiring board (PWB), making it a poor material for use in mechanical connections. These considerations lead to the conclusion that it will take a combined effort of researchers in mechanics and metallurgy to control the failures of these joints. A novel method of analysis must be developed to predict the remaining service life of the many SMT joints already in use.

A great deal of metallurgical information exists in the open literature describing the response of solder alloys subjected to thermomechanical loading [1]. However, the research systematically interpreting and documenting solder thermomechanical behaviors is relatively recent. Given the microstructural complexity of solder material, the majority of current methodologies are based on empirical curve fitting techniques. An additional serious drawback in the conventional methodology for solder joint analysis is the mandatory employment of different failure criteria with or without a

* This work was supported by the United States Department of Energy under Contract DE-AC04-94AL85000. Sandia is a multiprogram laboratory operated by Sandia Corporation, a Lockheed Martin Company, for the United States Department of Energy.

---

macro-crack. For instance, a plastic strain related failure criterion, like the Coffin-Manson relation [1], is often chosen to estimate the design life of a joint without a macro-crack under low stress or low cycle fatigue, while a different failure criterion such as the stress intensity factor K or the J-integral must be applied to characterize failure in a cracked joint. In essence, the approach employing a strain related failure criterion for an unnotched component is based on a "local" approach whereas a "global" approach is employed to characterize a "cracked" one. In the past decade, a new theory known as damage mechanics has been developed to a stage ready for a wide range of engineering applications [2-7]. The theory, which takes into account the gradual material degradation under continuous load application, is ideally suited for characterizing the aging of solder joints under cyclic thermomechanical loading. In addition, a unified failure criterion based on damage mechanics theory can be developed to predict the threshold conditions of damage evolution, crack initiation, and propagation in a material element with or without the presence of a macro-crack, which would not be possible using the conventional methodology.

The primary objective of our current research is to develop a comprehensive mechanics-based method of analysis capable of predicting the integrity and reliability of aging solder joints under thermomechanical loading. To achieve our goal, a fundamental understanding of the behavior of Sn-Pb solder alloy undergoing extensive irreversible plastic deformation must first be attained. Accordingly, a generalized formulation of damage characterization for solder material under substantial irreversible deformation is established. The characterization takes into account the effects of load history and plastic damage. In addition, the new constitutive equations are formulated in such a way that they can be readily incorporated into a general purpose finite element program such that the distributions of stress, strain, and plastic damage in a solder joint can be calculated and its fatigue life predicted.

2. DAMAGE MECHANICS MODELING

Damage is herein defined as gradual degradation or deterioration in a material element under continuous load applications. A measure of the material degradation may be quantified with an internal state variable $\mathbf{D}$. Accordingly, the relationship between effective stress and strain tensors and their respective Cauchy stress and strain tensors may be expressed as [2]

$$\tilde{\mathbf{S}} = \mathbf{M}(\mathbf{D}) : \mathbf{S} \tag{1}$$

$$\tilde{\mathbf{E}}^{\mathbf{e}} = [\mathbf{M}(\mathbf{D})^{-1}]^{\mathrm{T}} : \mathbf{E}^{\mathbf{e}} \tag{2}$$

where $\mathbf{S}$ is the Cauchy stress tensor, $\tilde{\mathbf{S}}$ the effective stress tensor, $\mathbf{E}^{\mathbf{e}}$ the elastic strain tensor, $\tilde{\mathbf{E}}^{\mathbf{e}}$ the effective elastic strain tensor, and $\mathbf{M}(\mathbf{D})$ the damage effect tensor of fourth order.

Based on the concept of strain energy equivalence of Chow and Lu [3], the elastic energy for a damaged material is the same as that of the undamaged material, when the stress and strain tensors are replaced by the corresponding effective parameters in the stress/strain based form. It may be expressed in the stress-based form as

$$W^{e}(\mathbf{S}, \mathbf{D}) = \frac{1}{2}\tilde{\mathbf{S}} : \mathbf{C}^{-1} : \tilde{\mathbf{S}} = \frac{1}{2}\mathbf{S} : \tilde{\mathbf{C}}^{-1} : \mathbf{S} \text{ and } \tilde{\mathbf{C}} = \mathbf{M}(\mathbf{D})^{-1} : \mathbf{C} : [\mathbf{M}(\mathbf{D})^{-1}]^{\mathrm{T}} \tag{3}$$

where $W^{e}(\mathbf{S},\mathbf{D})$ is the elastic complementary energy and $\mathbf{C}$ represents the fourth-order elastic compliance tensor of the virgin material. The constitutive equation of elasticity is derived from thermodynamic theory in terms of true stress and strain, and is expressed as

$$\mathbf{E}^{\mathbf{e}} = \frac{\partial W^{e}(\mathbf{S}, \mathbf{D})}{\partial \mathbf{S}} = \mathbf{C}^{-1} : \mathbf{S} \tag{4}$$

In the principal system of damage, the non-zero components in the matrix form of the damage effect tensor $\mathbf{M}(\mathbf{D})$ are expressed as

$$[M_{ij}(D)] = \begin{bmatrix} \frac{1}{1-D_1} & 0 & 0 & 0 & 0 & 0 \\ 0 & \frac{1}{1-D_2} & 0 & 0 & 0 & 0 \\ 0 & 0 & \frac{1}{1-D_3} & 0 & 0 & 0 \\ 0 & 0 & 0 & \frac{1}{1-\frac{1}{2}(D_2+D_3)} & 0 & 0 \\ 0 & 0 & 0 & 0 & \frac{1}{1-\frac{1}{2}(D_1+D_3)} & 0 \\ 0 & 0 & 0 & 0 & 0 & \frac{1}{1-\frac{1}{2}(D_1+D_2)} \end{bmatrix} \tag{5}$$

where D_1, D_2 and D_3 are the principal values of damage $\mathbf{D}$, which is a symmetric tensor of second order.

The evolution equations of plastic damage may be derived from the plastic damage energy release rate $\mathbf{Y_p}$, defined as

$$\mathbf{Y_p} = -\frac{\partial W^e(\mathbf{S},\mathbf{D})}{\partial \mathbf{D}} = -\mathbf{S} : \left(\tilde{\mathbf{C}}^{-1} : \mathbf{M}^{-1} : \frac{\partial \mathbf{M}}{\partial \mathbf{D}}\right)^s : \mathbf{S} \tag{6}$$

in which the superscript "*s*" means that only the symmetric part should be taken. The plastic damage criterion F_{pd} is assumed as

$$F_{pd} = Y_{peq}^{1/2} - [C_{p0} + C_p(Z)] = 0 \tag{7}$$

where C_{p0} is the initial strengthening threshold, $C_p(Z)$ the increment of the threshold, Z the equivalent overall damage, and Y_{peq} is defined as

$$Y_{peq} = \frac{1}{2}\mathbf{Y_p} : \mathbf{L_p} : \mathbf{Y_p} \tag{8}$$

$\mathbf{L_p}$ is the fourth-order characteristic tensor of plastic damage and its matrix form may be expressed as

$$[L_{pij}] = \begin{bmatrix} 1 & \eta_p & \eta_p & 0 & 0 & 0 \\ \eta_p & 1 & \eta_p & 0 & 0 & 0 \\ \eta_p & \eta_p & 1 & 0 & 0 & 0 \\ 0 & 0 & 0 & 2(1-\eta_p) & 0 & 0 \\ 0 & 0 & 0 & 0 & 2(1-\eta_p) & 0 \\ 0 & 0 & 0 & 0 & 0 & 2(1-\eta_p) \end{bmatrix} \tag{9}$$

where η_p is assumed to be a material constant defining the degree of damage anisotropy.

If the plastic damage criterion of Eq. 7 is taken as the potential function, the plastic damage evolution equations become

$$\dot{Z}_p = \lambda_{pd}\frac{\partial F_{pd}}{\partial(-C_p)} = \lambda_{pd} \tag{10a}$$

and

$$\dot{\mathbf{D}}_\mathbf{p} = \lambda_{pd}\frac{\partial F_{pd}}{\partial(-\mathbf{Y}_\mathbf{p})} = \frac{-\lambda_{pd}}{2Y_{peq}^{1/2}}\mathbf{L}_\mathbf{p} : \mathbf{Y}_\mathbf{p} \tag{10b}$$

where Z_p is the equivalent plastic damage and $\mathbf{D}_\mathbf{p}$ is the plastic damage tensor. The Lagrange multiplier λ_{pd} can be evaluated, based on Eq. 7, as

$$\lambda_{pd} = \frac{\frac{\partial F_{pd}}{\partial \mathbf{S}} : \dot{\mathbf{S}} + \frac{\partial F_{pd}}{\partial \mathbf{D}} : \dot{\mathbf{D}}}{\left(\frac{\partial F_{pd}}{\partial C_p}\right)^2 \frac{\partial C_p}{\partial Z}} > 0 \ , \ \text{if } F_{pd} = 0 \text{ and } \frac{\partial F_{pd}}{\partial \mathbf{S}} : \dot{\mathbf{S}} + \frac{\partial F_{pd}}{\partial \mathbf{D}} : \dot{\mathbf{D}} > 0 \tag{11a}$$

or

$$\lambda_{pd} = 0 \ , \ \text{if } (F_{pd} < 0) \text{ or } (F_{pd} = 0 \text{ and } \frac{\partial F_{pd}}{\partial \mathbf{S}} : \dot{\mathbf{S}} + \frac{\partial F_{pd}}{\partial \mathbf{D}} : \dot{\mathbf{D}} \le 0) \tag{11b}$$

When the yield criterion of a material with damage F_p is defined as

$$F_p(\mathbf{S}, \mathbf{D}, R) = F_p(\tilde{\mathbf{S}}) - [R_o + R] = 0 \tag{12}$$

where R_o and R are initial and increment strain hardening thresholds, respectively, the constitutive plastic equations incorporating material damage may be derived by taking Eq. 12 as the potential function. The plastic strain tensor $\mathbf{E}_\mathbf{p}$ and the equivalent plastic strain, p, are therefore determined by the following equations

$$\dot{\mathbf{E}}_\mathbf{p} = \lambda_p\frac{\partial F_p}{\partial(\mathbf{S})} \tag{13a}$$

and

$$\dot{p} = \lambda_p\frac{\partial F_p}{\partial(-R)} = \lambda_p \tag{13b}$$

in which λ_p is determined by

$$\lambda_p = \frac{\frac{\partial F_p}{\partial \mathbf{S}} : \dot{\mathbf{S}} + \frac{\partial F_p}{\partial \mathbf{D}} : \dot{\mathbf{D}}}{\left(\frac{\partial F_p}{\partial R}\right)^2 \frac{\partial R}{\partial p}} > 0 \ , \ \text{if } F_p = 0 \text{ and } \frac{\partial F_p}{\partial \mathbf{S}} : \dot{\mathbf{S}} + \frac{\partial F_p}{\partial \mathbf{D}} : \dot{\mathbf{D}} > 0 \tag{14a}$$

or

$$\lambda_p = 0 \ , \ \text{if } (F_p < 0) \text{ or } (F_p = 0 \text{ and } \frac{\partial F_p}{\partial \mathbf{S}} : \dot{\mathbf{S}} + \frac{\partial F_p}{\partial \mathbf{D}} : \dot{\mathbf{D}} \le 0) \tag{14b}$$

3. DETERMINATION OF DAMAGE PARAMETERS AND VERIFICATION

The proposed damage model calls for the determination of a number of damage variables which are considered as intrinsic material properties required as the finite element input for predicting damage behaviors of solder joints. The solder material chosen for the investigation is the typical 60Sn-40Pb due to its importance in electronic applications. The material is assumed to be initially isotropic. To demonstrate the application of the damage mechanics characterization developed in the preceding section, the damage behavior analyses for the solder joint material under uniaxial tension and pure shear are performed.

Under uniaxial stress σ_1, from Eqs. 4, 7, and 10, one has the following equations,

$$\tilde{E}_1 = E_1(1-D_1)^2\,,\quad \tilde{\nu}_{12} = \nu_{12}\frac{(1-D_1)}{(1-D_2)}\,,\quad Y_{peq}^{1/2} = \frac{\sigma_1^2}{\sqrt{2}E_1(1-D_1)^3} \tag{15a}$$

$$dD_1 = \frac{\sqrt{2}(1-D_1)\sigma_1 d\sigma_1}{2E_1(1-D_1)^4\dfrac{\partial C_p}{\partial Z} - 3\sigma_1^2}\,,\quad D_2 = \eta_p D_1\,,\quad Z = \sqrt{2}D_1 \tag{15b}$$

where $\tilde{E}_1$ and $\tilde{\nu}_{12}$ are the effective elastic modulus and Poisson's ratio, respectively.

A series of uniaxial tests for standard tensile specimens has been conducted to measure the effective elastic modulus, the effective Poisson's ratio, and the true stress-strain curve, which are in turn used to determine the plastic damage variables and their associated damage parameters. The specimen geometry is shown in Fig. 1 in accordance with the ASTM E8-93a standard. On the specimens, light machining grids l_o of 0.0394 inch division were made within the gauge length L_o of 2.9 inch for the purpose of plastic strain measurement.

The experiments were conducted with an electro-hydraulic servo-controlled MTS 810 at room temperature. The dimension of each specimen was measured with a vernier caliper within an accuracy of 0.001 inch. The specimens were loaded incrementally under displacement control at different loading rates. In determining the effective Young's modulus before necking, the total strains are measured with an extensometer (model MTS 632.12B-20). Upon unloading, the plastic strain was measured by recording the spacing between specimen marks with a direct measuring microscope of

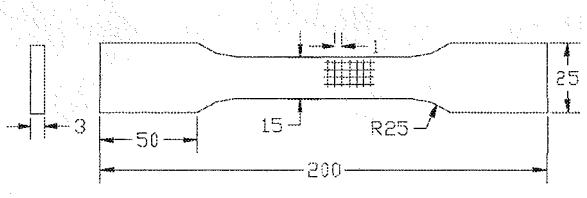

Fig. 1 Tension test specimen (all unit: mm)

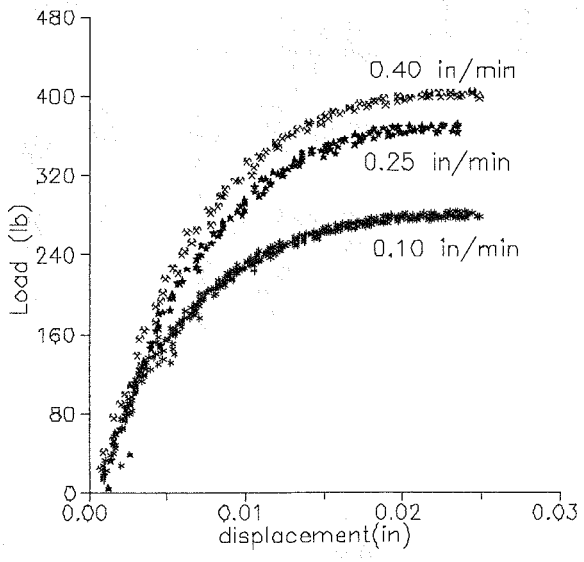

Fig. 2 Load-displacement curves at 3 rates

20 magnification with 0.0025 inch divisions. In evaluating the effective Young's modulus after necking, the strain upon reloading was measured with a strain gauge indicator (model P-3500) from strain gauges (type: FCA-2-11 rosette, resistance: $120.0 \pm 0.5\Omega$, gauge factor: $2.12 \pm 1.0\%$, manufactured by TML Tokyo Sokki Kenkyuju Co., Ltd.). The strain gauges and strain indicator were also used to measure the transverse strain under uniaxial tension to obtain initial and effective Poisson's ratios.

The deformation behavior of the specimen consists of three distinct phases, namely, uniform deformation, localized necking, and final rupture. At the initial loading when deformation is uniform, only spacing L_i between the first line and the last line, i.e., the current gauge length, needed to be measured, and the true strain is evaluated using

$$\varepsilon = \ln(L_i/L_o)$$

However, when localized plastic deformation in the necking area has occurred, spacing between two neighboring marks l_i is measured within the necking zone, and the true strain is calculated with

$$\varepsilon = \ln(l_i/l_o)$$

The variation of specimen width and thickness are also recorded to obtain the true stress as

$$\sigma = P_{app}/A$$

where P_{app} is the applied load and A the current cross-section area.

Fig. 2 depicts the load-displacement curves of the 60Sn-40Pb material at different loading rates. For the sake of illustration, the measured true stress-strain relationship at the rate of 0.25 inch/min is shown in Fig. 3. The measurement of the effective Young's modulus and Poisson's ratio enables the determination of the damage variable D_1 and D_2 from Eq. 15a. At the same loading rate, Fig. 4 illustrates the measured changes of effective Young's modulus and Poisson's ratio with strains, revealing, as expected, gradual material degradation with increase in strain. Evolution of damage variables D_1 and D_2 with strain at the rate of 0.25 inch/minute are shown in Fig. 5, indicating some degree of plastic damage anisotropy at high strain. This confirms that the proposed damage coefficient of $\mathbf{L_p}$ should provide a good approximation to the actual damage progression. The value of parameter η_p in Eq. 8 is then determined from these curves to be 0.834. The increment of plastic damage threshold C(Z) can also be readily evaluated experimentally as a function of the equivalent plastic damage as shown in Fig. 6.

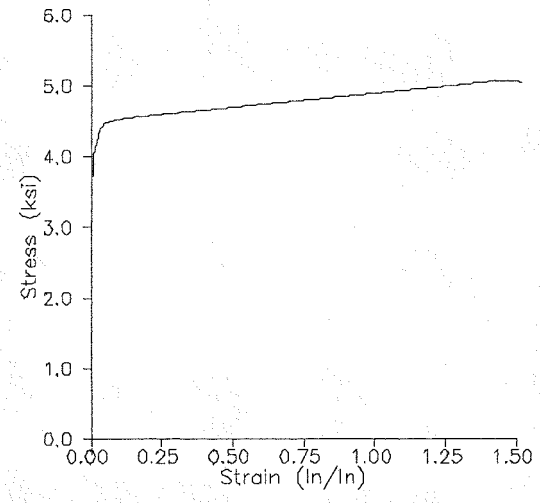

Fig. 3 Stress-strain curve for 0.25 in/min

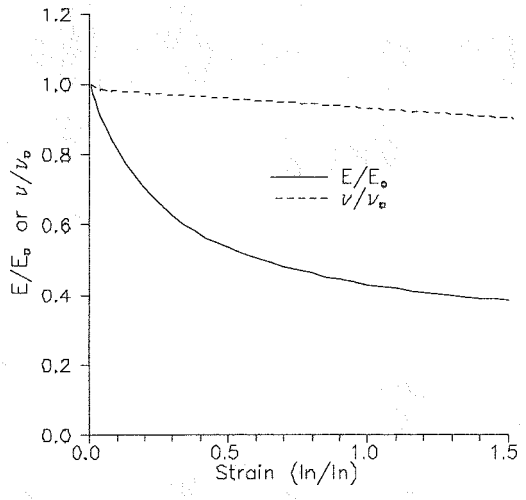

Fig. 4 Variation of E/E_o and ν/ν_o with strain

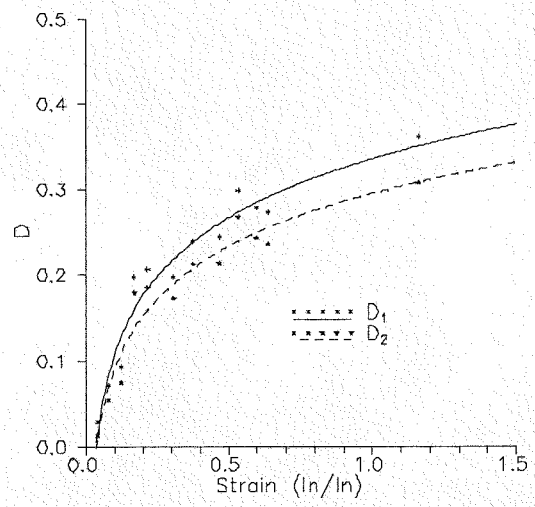

Fig. 5 Evolution of damage with strain

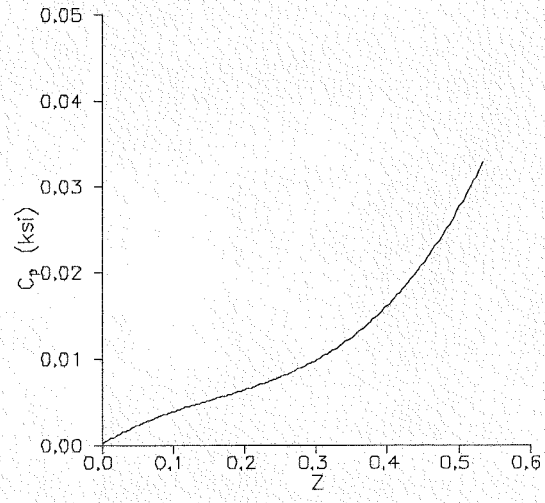

Fig. 6 C_p-Z curve

In order to conduct a validation analysis for the proposed damage model described in the preceding sections, a series of pure shear experiments were also performed at room temperature. The specimen shown in Fig. 7 was prepared, using the same material as the one for uniaxial testing, in accordance with the ASTM B831-93 standard for pure shear test. One of the shear test results is presented in Fig. 8, which shows a crack was forming during the test. To predict the ultimate shear strength of the material analytically, the plastic damage parameters determined under the uniaxial load were used as input data. The slope $\partial C_p/\partial Z$, required in Eq. 15b, was obtained from the curve given in Fig. 6. The critical value of equivalent overall damage Z_{cr}, which is used to determine the material final failure, was found to be 0.53 according to the value of D_1 shown in Fig. 5 and the expression of Z given in Eq. 15b. From Eqs. 9 and 10, the predicted shear ultimate strength for the specimen shown in Fig. 7 is 3.12 ksi, which compares satisfactorily with the experimental value of 2.84 ksi, resulting in a discrepancy of 9% between model and experiment. The result of shear stress analysis is encouraging since it confirms the validity and accuracy of the damage model for pure shear loading, which is considered to be the predominant stress mode for solder joints.

4. CONCLUSIONS

This paper presents a method of damage mechanics analysis for eutectic 60Sn-40Pb solder alloy undergoing substantial irreversible plastic deformation. As real-life engineering materials, such as the solder alloy, contain varying degrees and sizes of defects in the form of cracks/voids, the conclusions derived from classical methods of analysis, which assume materials to be perfect or free of defects, become suspect. The theory of damage mechanics, however, takes into account the gradual material degradation or deterioration resulting from the initiation, growth and coalescence of micro-cracks/voids in a material element. The material degradation may be caused by continuous load application, aging or cyclic loading of the eutectic alloy.

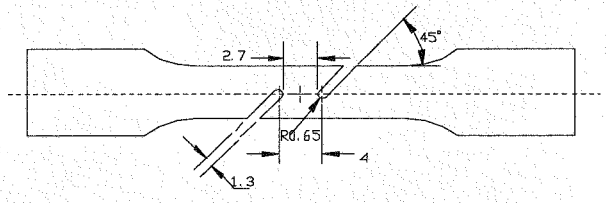

Fig. 7: Shear test specimen (all unit: mm)

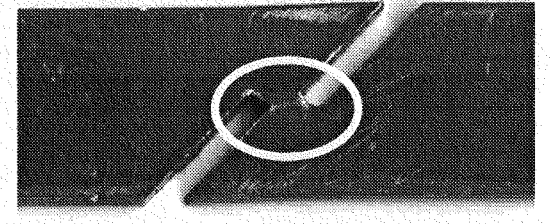

Fig. 8: A crack formed under shear test

The constitutive equations of elastic and plastic coupled damage are first derived. The damage strain energy release rate is then formulated and used to develop the damage evolution equation. As shear mode of fracture is often observed in solder joints, the proposed damage model is applied to predict shear fracture. Before the validation analysis can be carried out, a series of tests are performed to determine the required damage variables under three loading rates of 0.1 in/min, 0.4 in/min and 0.25 in/min. The results confirm the rate dependent property of the material. The measured damage variables are then used to determine the true stress and strain as well as the progressive material degradation in terms of effective Young's modulus and Poisson's ratio. The measured damage parameters are then applied to calculate shear fracture stress which compares favorably with that measured experimentally. The comparison confirms the validity of the proposed damage model to characterize shear fracture in solder joint material.

Solder joints in real life are subjected to a combination of thermal and mechanical cycling. In addition, the material exhibits significant strain-rate dependency at operating temperatures. Therefore, a program to extend the current damage mechanics model and characterization to include the effects of temperatures, strain rates, fatigue, and creep damages in Sn-Pb solder joint material is being actively pursued, and preliminary results have shown promise.

ACKNOWLEDGEMENT

C. L. Chow and Fan Yang wish to gratefully acknowledge support of this research through a contract with Sandia National Laboratories.

REFERENCES

1. D. R. Frear, S. N. Burchett, H. S. Morgan, & J. H. Lau, *The Mechanics of Solder Alloy Interconnects*, Van Nostrand Reinhold, New York, 1994.
2. C. L. Chow and J. Wang, International Journal of Fracture, 33 (1987), 3-16.
3. C. L. Chow and T. J. Lu, Engineering Fracture Mechanics, 34 (1989), 679.
4. C. L. Chow and J. Wang, Engineering Fracture Mechanics, 27 (1987), 547-558.
5. C. L. Chow and J. Wang, Damage Mechanics in Composites, ASME, AD-12 (1987), 1-10.
6. C. L. Chow and J. Wang, International journal of fracture, 38 (1988), 83-102.
7. L. G. Yu, Ph.D. Dissertation, The University of Hong Kong, 1993.